

# Pontoon and Membrane Breakwater

S.T. Kee\*

\*Civil Engineering Dept. Seoul national University of Technology, Seoul, Korea

**KEY WORDS:** floating pontoon, porous membrane, floating flexible breakwater, hydroelasticity, multi-domain BE

**ABSTRACT:** A numerical study on the hydrodynamic properties of a floating flexible breakwater consisting of triple vertical porous membrane structures attached to a floating rigid pontoon restrained by moorings is carried out in the context of two-dimensional linear wave-flexible body interaction theory. The tensions in the triple membranes are achieved by hanging a clump weight from its lower ends. The clump weight is also restrained properly by moorings. The dynamic behavior of the breakwater was described through an appropriate Green function, and the fluid multi-domains are incorporated into the boundary integral equation. Numerical results are presented which illustrate the effects of the various wave and structural parameters on the efficiency of the breakwater as a barrier to wave action. It is found that the wave reflection and transmission properties of the structures depends strongly on the membrane length taking major fraction of water column, the magnitude of tensions on membrane achieving by the clump weight, proper mooring types and stiffness, the permeability on the membrane dissipating wave energy.

## 1. Introduction

Flexible membranes offer an attractive means of providing temporary protection from waves in semi-protected regions. In addition, it has desirable characteristics of being lightweight, transportable, reusable, relatively inexpensive, and rapidly deployable (Thomson et al. 1992). Thus, it may be an ideal candidate as a portable/ temporal breakwater for the protection of various coastal/offshore structures and sea operations requiring relatively calm sea states (e.g. Fowler et al, 1996).

Aoki et al. (1994) have provided a theoretical solution for bottom-mounted, sub-merged, membrane structure in waves. The hydrodynamic characteristics of various buoy/membrane systems that vertical flexible membranes are attached to the floating buoys are investigated by Kim & Kee (1996), Kee & Kim (1997), Cho et al. (1997, 1998).

Kee (2001a, b), Cho & Kim (2000), Kee (2002) have studied the oblique wave interaction with buoy/porous-membrane, horizontal porous-membrane, and horizontal/vertical porous-membrane.

Kee et al. (2001) numerically investigated the hydrodynamics properties of triple vertical-porous-membranes interacting with linear oblique waves. The triple vertical porous membranes hinged at the beneath of the pontoon that is water surface pierced and fixed for simplicity. Those membranes are extended downward and hinged at some distances from seabed, which can allow the passage of sediment.

In this paper, the performance as wave barrier to wave action and the motions of pontoon and clump weight restrained by mooring lines are numerically investigated. The fluid motion in the multi-sub fluid domains is idealized as linearized, two-dimensional potential flow and the equation of motion of inextensible and porous membrane is taken to be that of a one-dimensional membrane of uniform mass per unit length subject to a constant tension. The pontoon that provides required a large initial constant tension on the membrane is assumed to be rigid and uniformly long in the longitudinal direction so that two-dimensional analysis can be applied. In addition, it is also assumed the heave motion of floating structure is negligible for simplicity due to large initial tension of membranes.

The solution of such complicated hydroelasticity problems with a rigid body can be obtained by solving the following three problems simultaneously. First, the hydrodynamic interaction of oblique incident waves with a rigid body and multi-layer porous-flexible bodies was solved

---

#172, Kongneung-dong, Nowon-Gu, Seoul, Korea(139-743)

02-970-6509 stkee@snut.ac.kr

by the distribution of the simple sources (modified Bessel function of the second kind) that satisfy the Helmholtz governing equation. Second, the interaction of the pontoon and triple membranes is taken into consideration through appropriate boundary conditions at three hinges beneath the pontoon. Third, the velocity potentials of wave motion are fully coupled with triple porous membrane deformations and viscous damping due to porosities based on Darcy's law. The theory and numerical results are validated through energy relation for non-porous cases and conversance tests for various porosities. Using the developed four-domain boundary integral techniques, the performance with various parameters of the pontoon and porous membranes are thoroughly examine

## 2. Theory and Numerical Methods

We consider the interaction of a floating pontoon with vertical triple porous membrane wave barriers with obliquely incident waves. The membranes can be hinged at the beneath of pontoon and tip of a floating clump weight that is composed of steel frames restrained by moorings. Assuming ideal fluid and harmonic motion of frequency ( $\omega$ ), the velocity potential of an oblique monochromatic wave can be written as  $\Phi(x, y, z, t) = Re[\phi(x, y) e^{i k_z z - i \omega t}]$ , where  $k_z = k_0 \sin \theta$  is the wave number component in the  $z$  direction and  $\theta$  is the angle(wave heading) of a plane monochromatic incident wave of amplitude  $A$ , wavenumber  $k_0$ , and wave heading ( $\theta$ ) is given by

$$\phi_o = \frac{-igA}{\omega} \frac{\cosh k_o(y+h)}{\cosh k_o h} e^{i k_x x} \quad (1)$$

where  $k_x = k_o \cos \theta$ ,  $\omega^2 = k_o g \tanh k_o h$  with  $g$  and  $h$  being the gravitational acceleration and water depth, respectively. The complex velocity potentials,  $\phi_1$ ,  $\phi_2$ ,  $\phi_3$  and  $\phi_4$ , in four fluid domains 1, 2, 3 and 4 (see Fig. 1), then satisfy the Helmholtz equation  $\nabla^2 \phi_l - k_z^2 \phi_l = 0, (l=1, 2, 3, 4)$  as governing equation and the following linearized free-surface ( $\Gamma_F$ ), bottom ( $\Gamma_b$ ), and radiation condition:

$$-\omega^2 \phi_l + g \frac{\partial \phi_l}{\partial y} = 0 \quad (\text{on } \Gamma_F) \quad (2)$$

$$\frac{\partial \phi_l}{\partial n} = 0 \quad (\text{on } \Gamma_b) \quad (3)$$

$$\lim_{|x| \rightarrow \infty} \left( \frac{\partial}{\partial x} \pm i k_x \right) (\phi_l - \phi_o) = 0 \quad (\text{on } \Gamma_c) \quad (4)$$

where  $\Gamma_c$  is the vertical truncation boundaries at far fields and  $n = (n_x, n_y)$  is the unit outward normal vector. Along the vertical matching boundaries in fluids at  $x = -W/2, 0, +W/2$ , the pressure and normal velocity are required to be continuous as follows;

$$\phi_l - \phi_{l+1}, \quad \frac{\partial \phi_l}{\partial x} = -\frac{\partial \phi_{l+1}}{\partial x} \quad \text{at } \Gamma_f \quad (5)$$

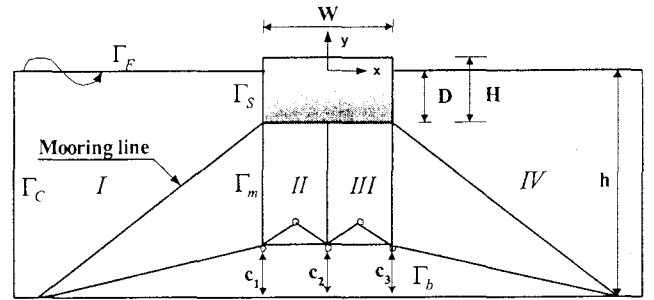


Fig. 1. Coordinate system and integration domains

The scattered potentials must satisfy the following linearized kinematic boundary conditions on the membrane surface based on Darcys law that the normal velocity inside of membrane with fine pores is linearly proportional to the pressure difference between the two sides of the membrane (Wang & Ran 1993).

$$\frac{\partial \phi_l}{\partial x} = -\frac{\partial \phi_{l+1}}{\partial x} = -i\omega \xi + \frac{B}{\mu} \rho i \omega (\phi_l - \phi_{l+1}) \quad (6)$$

where  $\mu$  is constant coefficient of dynamic viscosity,  $\rho$  is constant fluid density, and  $B$  is a material constant called permeability having the dimension of a length, and the harmonic membrane motions  $(y, t) = Re[\xi(y) e^{i k_z z - i \omega t}]$ . For simplicity, the heave motion of the buoy is assumed to be negligible under large initial tension of membrane. Then the boundary condition on the floating buoy is

$$\frac{\partial \phi_l}{\partial n} + i\omega(\eta_1 n_x + \eta_3 n_\theta) + \frac{\partial \phi_o}{\partial n} = 0, l=1, 2, 3, 4 (\text{on } \Gamma_B) \quad (7)$$

where  $n_\theta = x n_y - y n_x$  and the symbols  $\eta_1$  and  $\eta_3$  represent complex sway and roll responses. To solve the present boundary value problem, a four-domain boundary integral equation method using simple sources along the entire boundary is developed, which can be used for arbitrary bottom topography.

Applying Green's second identity in each of the domains to the unknown potentials  $\phi_l$  and imposing the relevant boundary conditions Eqs. 2-7, the integral equations in each fluid domain can be written as

$$\begin{aligned}
& C\phi_l + \int_{\Gamma_l} \left[ k_z K_1(k_z r) \frac{\partial r}{\partial n} - \nu K_0(k_z r) \right] \phi_l d\Gamma + \\
& \int_{\Gamma_l} \left[ k_z K_1(k_z r) \frac{\partial r}{\partial n} - ik_x K_0(k_z r) \right] \phi_l d\Gamma + \\
& \int_{\Gamma_h} \left[ \phi_l k_z K_1(k_z r) \frac{\partial r}{\partial n} d\Gamma + i\omega K_0(k_z r) (\eta_1 n_x + \eta_3 n_\theta) + \right. \\
& \left. K_0(k_z r) \frac{\partial \phi_0}{\partial n} \right] d\Gamma + \\
& \int_{\Gamma_m} \left[ \phi_l \left\{ k_z K_1(k_z r) \frac{\partial r}{\partial n} - s_l \frac{B}{\mu} i\rho\omega K_0(k_z r) \right\} + \right. \\
& \left. s_l \frac{B}{\mu} i\rho\omega K_0(k_z r) \phi_{l+1} + s_l (i\omega \xi_i) K_0(k_z r) \right] d\Gamma + \\
& \int_{\Gamma_h} \phi_l K_z K_l(K_z r) \frac{\partial r}{\partial n} d\Gamma = 0 \quad (l=1, 2, 3, 4) \quad (8)
\end{aligned}$$

where  $C$  is solid-angle constant, and  $\nu = \omega^2/g$  is the infinite-depth wave number,  $s_l = 1, s_4 = -1$ .  $K_0$  and  $K_l$  is the modified zeroth-order and first order Bessel function of the second kind and  $r$  is the distance from the source point  $(x', y')$  to the field point  $(x, y)$ . In fluid domain [II,III] and [III,VI] backward side of front membrane and forward side of rear membrane is coexist with each same spacing ( $W/2$ ). Thus, in domain [II,III] and [III,VI],  $s_2 = s_3 = -1$ , and  $s_2 = s_3 = 1$  are for backward side of front membrane and forward side of rear membrane respectively.

The disturbance potentials must satisfy the following linearized dynamic boundary conditions on the membrane surface such as the discrete form of each equation of membrane motions for  $j$ -th element;

$$\begin{aligned}
& \rho i\omega (\phi_{(j)} - \phi_{(j+1)}) (l_j) - T_{(j)} \left( \frac{\partial \xi_i}{\partial \zeta} \right)_j + T_{(j+1)} \left( \frac{\partial \xi_i}{\partial \zeta} \right)_{j+1} \\
& = -m l_j \omega^2 (\xi_i)_{(j)} \text{ on } \Gamma_m \text{ and } i=1, 2, 3 \quad (9)
\end{aligned}$$

where  $(\partial \xi_i / \partial \zeta)_j = (\xi_i)_j - (\xi_i)_{j-1} / (\Delta \zeta)_j$ ,  $(l_j)$  is the length of the  $j$ -th segment of each membrane, and  $(\Delta \zeta)_j = \{ (l_j) + (l_j)_{(j+1)} \} / 2$ .

The geometric boundary conditions at the hinged points

and the top connection points of membrane are  $\xi_i = 0$  at  $y_i = -(h - c)$ ,  $\xi_i = \eta_1 + R_i \eta_3$  at  $y_i = -D$ .  $R_i$  is a distance from each connection point of membrane to rotation center of pontoon.

Next, we consider the rigid-body motion of a buoy. As mentioned before, it is assumed that the heave response is negligible due to large initial tension. The coupled equations of motion for sway and roll are given by

$$M(-\omega^2)X = F_p - (K_{HS} + K_m)X - \sum_{I=1}^3 (F_T)_I \quad (10)$$

where  $X$  is displacement of sway and roll,  $M$  is a mass matrix of pontoon,  $F_p$  is hydrodynamic forces and moments on pontoon,  $K_{HS}$  is the restoring forces and moments due to the hydrostatic pressure,  $K_m$  is sway and roll mooring stiffness coefficients including the effects of pretension. The symbol  $(F_T)_I, (I=1, 2, 3)$  is forces and moments on the pontoon caused by the initial tension of membranes at the connection points between membranes and pontoon.

$$(F_T)_I = (T_i)_{(N_m+1)}$$

$$\left\{ \begin{array}{l} -\sin \alpha_i \\ R_i \cos(\beta_i + s_i \eta_3) \cos \alpha_i - R_i \cos(\beta_i + s_i \eta_3) \sin \alpha_i \end{array} \right\} \quad (11)$$

where  $\alpha_i$  is angles of membrane at the connections with respect to the  $y$  axis and the symbol  $R_i$  is the radial distances from the center of rotation of pontoon to each connection point on pontoon,  $s_1 = s_2 = -1, s_3 = +1$ , and  $\beta_i$  is angles of membrane at the connections with respect to center of rotation of pontoon.

So far, we have obtained integral equation (Eq. 8) for  $\phi_l, l=1, 2, 3, 4$ , and equation of membrane motion  $\xi_l$  and equations of pontoon motions  $\eta_1$  (sway),  $\eta_3$  (roll) (Eq. 10). They are mutually coupled, so they need to be solved simultaneously. If we discretize fluid domain 1 and 4 by  $NE_{1.4}$  segments, and domains 2, 3 by  $NE_{2.3}$ , we have  $2 NE_{1.4} + 2 NE_{2.3}$  unknown for  $\phi_l (l=1, 2, 3, 4)$ ,  $3 N_m$  unknown for  $\xi_i (i=1, 2, 3)$  and two unknown motions  $(\eta_1, \eta_3)$  of a floating pontoon. Therefore,  $NT = 2 NE_{1.4} + 2 NE_{2.3} + 3 N_m + 2$  number of linear simultaneous equations has to be solved for a floating pontoon with membranes hinged at some distance from the sea bed.

### 3. Numerical Results and Discussions

The four-domain boundary element program developed as described in the preceding section was used to demonstrate the performance of a floating pontoon/membrane wave barrier that is restrained properly with linear moorings in oblique incident waves. The computational domain is defined as in Fig. 1. The vertical truncation boundary is located 3-4 water depth away from the edge of a floating structure to ensure that local wave effects are negligible. The numerical results were checked against the energy-conservation formula for non-porous system, and convergence test for various porous coefficients.

The performance of the floating pontoon/triple membranes system as wave barrier depends upon several parameters, water depth, the width, draft, height of pontoon, and clearance between the bottom of system and sea, denoted by  $h, W, D, H, c$  and the excess buoyancy of the system, mooring line stiffness, and permeability of membranes,  $T, T/K$ , and  $B$ , respectively. The toe angle of mooring attached to the side of pontoon is The floating pontoon/membrane system allows exactly same spacing between membranes and bottom clearances between the hinged points and sea floor  $c_i, i=1, 2, 3$  for each region. The convergence test of the developed BEM program has been conducted for the porous or non-porous test system with design parameters  $W/h=0.5, H/h=0.25, T/K=0.1$  (mooring type 3 as show in Fig. 8.),  $D/h=0.2, c_i/h=0.0625$ , and  $\theta=0^\circ$ .

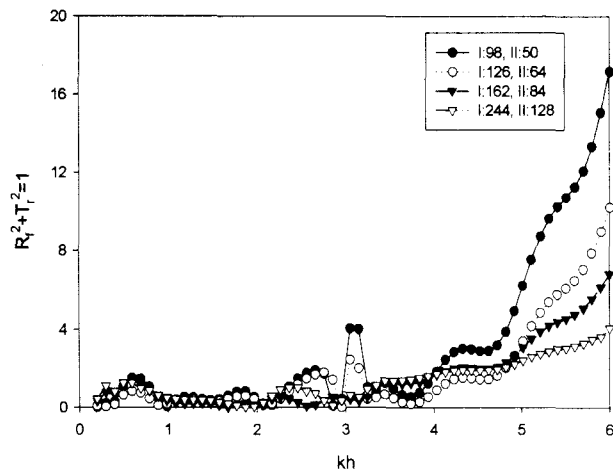


Fig. 2. Energy Relation for a system with non porous membrane

Fig. 2 shows that the energy relation is satisfied under the error of 4% along the whole non-dimensional wave number  $kh$  for non-porous system. Fig. 3 shows the convergence of reflection coefficient for porous system with permeability of

$B=1E-7$  as increasing the number of segments in outer and inner fluid domains. From those tests, the number of total elements in the outer/inner fluid domain  $N=244,128$  gave sufficient accuracy, and thus was used for the ensuing further computation.

The Fig. 4 show the transmission coefficients against various permeability coefficients for a test system. It is interesting to note that the higher porosity coefficient smudges the choppy spikes of transmission coefficients along whole the non-dimensional wave frequency. Thus the performance for higher permeability coefficient can be better or worse against corresponding frequency bands, especially better around  $0.8 \leq kh \leq 2.2, kh \geq 3.8$  and worse on  $kh \approx 0.5, 2.2, 3.3$

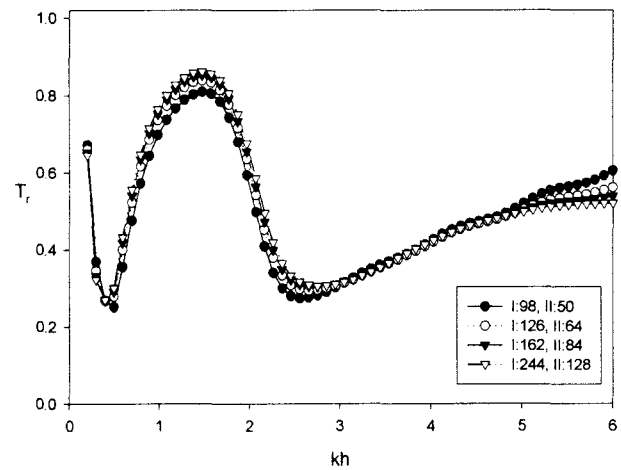


Fig. 3. Convergence of transmission coefficients for a system with porous membrane and for  $B = 1E - 7$

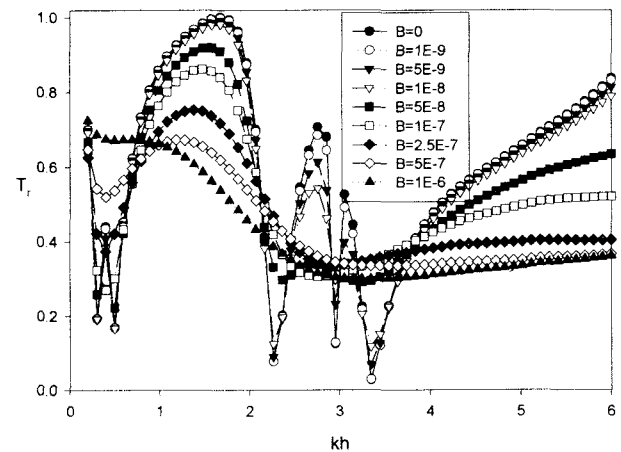


Fig. 4. Transmission coefficients of various permeability B

The transmission coefficient and non-dimensional sway displacement of pontoon and clump weight normalized by wave amplitude for a porous test system with varying mooring line stiffness and are shown in Fig. 5, Fig. 6 and Fig 7. As the mooring line stiffness is increased, the transmission coefficients and sway motions of pontoon and clump weight respectively are gradually decreased along the all frequency as intuitively expected. The performance based on transmission coefficient is significantly enhanced on the higher wave frequency region on  $3.0 \leq kh$  as the strong mooring line stiffness is increased. However, the effects of mooring stiffness on the performance are not significant for the lower frequency range when it compared to that of higher frequency range.

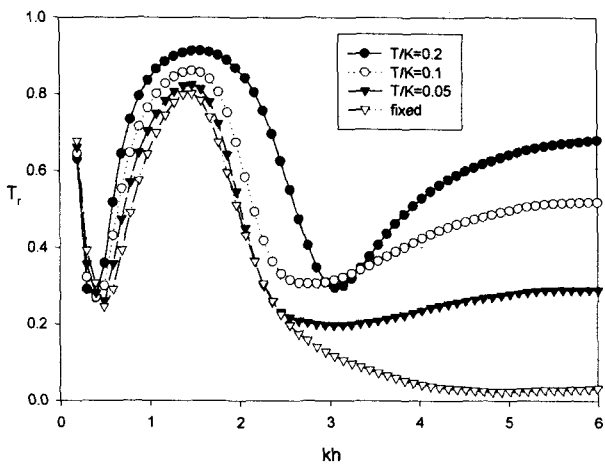


Fig. 5. Transmission coefficients of various mooring stiffness

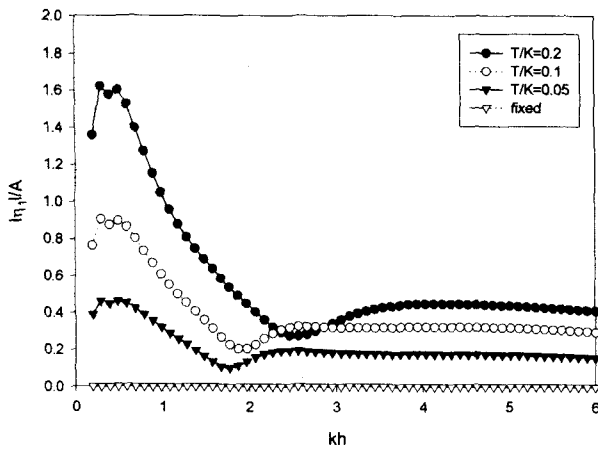


Fig. 6. Sway motion of a pontoon for various mooring stiffness

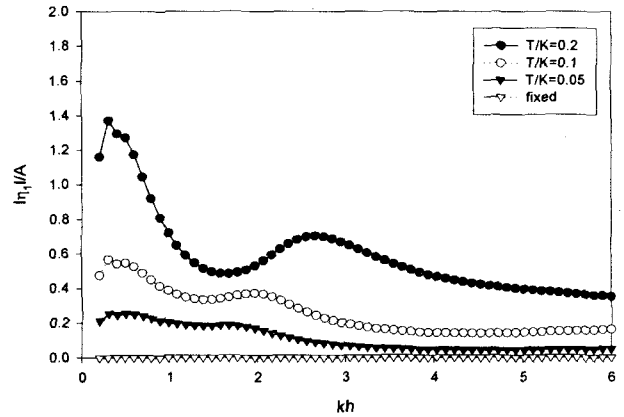
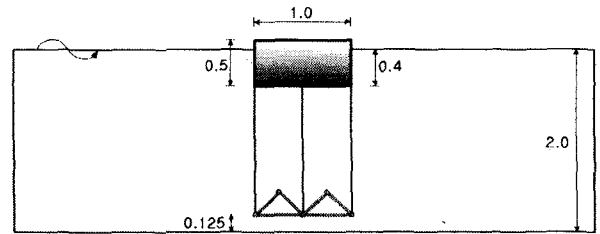
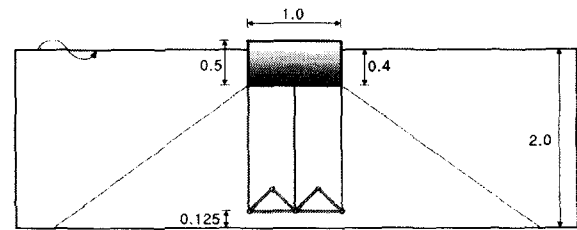


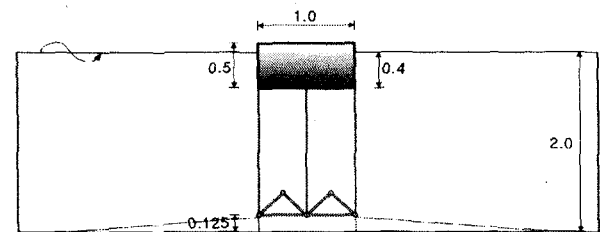
Fig. 7. Sway motion of a clump for various mooring stiffness



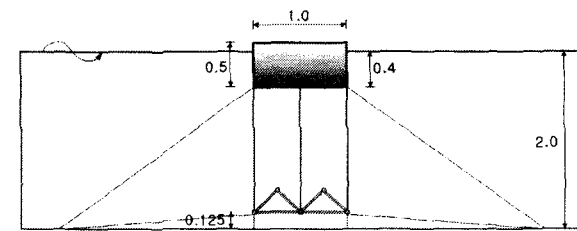
no mooring



type 1



type 2



type 3

The various mooring types applied to the floating pontoon membrane breakwater are depicted in Fig. 8. The transmission coefficient for various mooring type with stiffness  $T/K=0.1$  for all moorings are shown in Fig. 9. The effects to the performance as breakwater by mooring type2 are slightly improved compare to that of no mooring around lower frequency range; however, it is worse on the higher frequency range. The other mooring types show the much improved performance along the wide frequency range compared to that of the previous no mooring and type2.

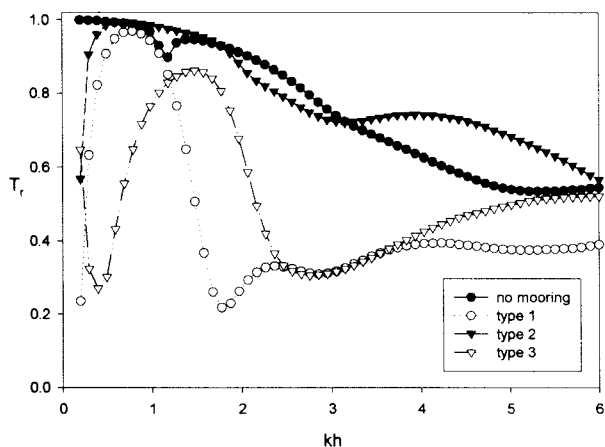


Fig. 9. Transmission coefficient of various mooring types

The effects of various pontoon drafts or widths on the transmission coefficients are shown in Fig. 10 and Fig. 11. It can be seen that the breakwater system consisting of deeper draft or wider floaters has, as intuitively expected, better efficiency as a wave barrier. However, the reversed trend appears around the non-dimensional frequency of  $1.5 \leq kh \leq 2.5$ . In particular, it is noted that the transmission coefficient associated with the shallow draft pontoon exhibits higher wave transmission along the low frequency range. The widest test model with  $W/h=1$  has excellent performance along the whole frequencies except the range of  $2.2 \leq kh \leq 3$

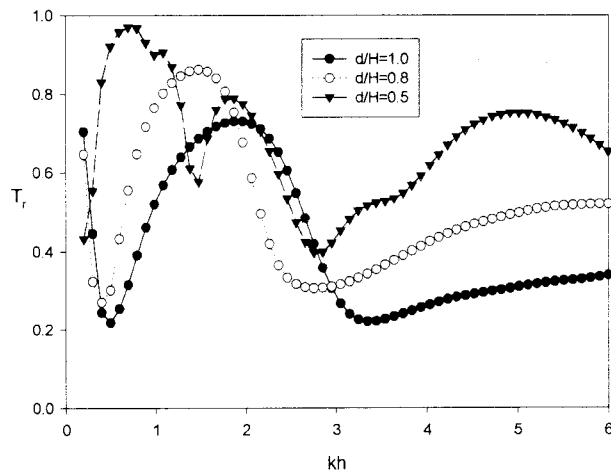


Fig. 10. Transmission coefficient of various drafts of pontoon

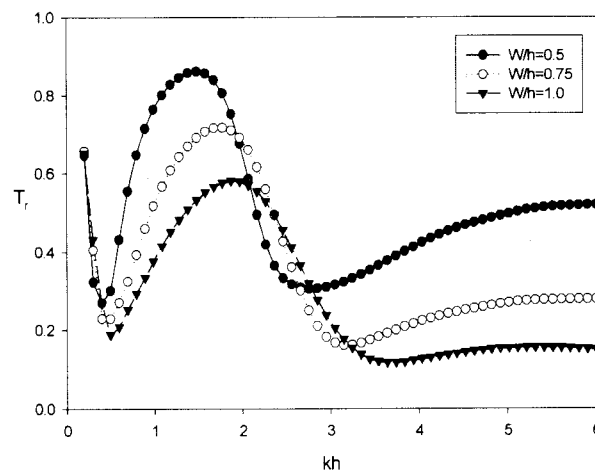


Fig. 11. Transmission coefficient of various width of pontoon

The transmission coefficient for the varying incident wave heading for a test system with porosity same  $B=2.5E-7$  on triple membranes is shown in Fig. 12. The performance as wave barrier is generally excellent for the wide range of frequency and wave headings except possible resonance frequency around  $kh = 1.5$

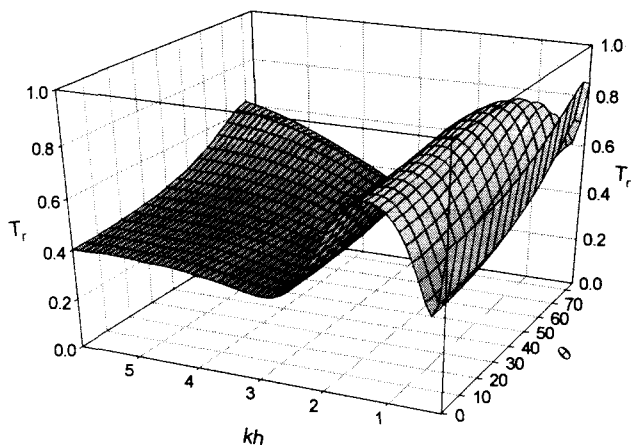


Fig. 12. Transmission coefficient for various wave headings and a porous test system with  $B = 2.5E - 7$ .

#### 4. Summary and Conclusion

A two-dimensional boundary integral method has been developed for the four-fluid sub domains split by triple vertical thin membranes. Using the developed program code, the performance of the floating pontoon with multiple porous membranes in oblique waves was tested for various breakwater design parameters, wave conditions, and permeability. From these results analysis, it is shown that the multiple porous membranes system can significantly increase the overall wave blocking efficiency in normal and oblique incident waves. The deeper draft of pontoon or wider pontoon enhances the wave blocking efficiency along the wide range of frequency.

#### Acknowledgements

This research was sponsored by the Korea Institute of Construction Technology (KICT) Research Center Program, Grant Number R&F/00-24-01.

#### Reference

- Aoki, S., Liu, H., & Sawaragi, T. (1994) "Wave transformation and wave forces on submerged vertical membrane" *Proc. Intl. Symp. Waves - Physical and Numerical Modeling*, Vancouver, 1287-1296
- Cho, I.H. & Kim, M.H. (2000). "Interactions of Horizontal Porous Flexible Membrane with Waves" *ASCE J. of Waterway, Port, Coastal & Ocean Engineering*, Vol.126, No.5, pp.245-253.

- Cho, I.H. & Kee, S.T. & Kim, M.H. (1998). "The Performance of Dual Flexible Membrane Wave Barrier in Oblique Sea" *ASCE J. of Waterway, Port, Coastal & Ocean Engineering*, Jan./Feb. 1998 Vol. 124, No.1, pp. 21-30.
- Cho, I.H. & Kee, S.T. & Kim, M.H. (1997). "The Performance of Dual Flexible Membrane Wave Barrier in Oblique Incident Waves" *J. of Applied Ocean Research*, Jun./Aug. 1997. Vol.19, No.3-4, pp.171-182.
- Fowler, J., Resio, D., Briggs, M., Pollock, C. (1996) "Potential uses for rapidly installed breakwater systems" *Proc. 12th ICCE Conf., Orlando*
- Kee, S.T. & Kim, M.H. (1997) "Flexible membrane wave barrier. Part 2. Floating/submerged buoy-membrane system" *ASCE J. of Waterway, Port, Coastal & Ocean Engineering*, Vol.123, No.2, 82-90.
- Kee (2001a) Performance of the submerged dual buoy/membrane breakwaters in oblique seas. *Journal of Ocean Engineering and Technology* Vol. 15, No 2, pp. 11-21.
- Kee (2001b) Resonance and response of the submerged dual buoy/porous-membrane breakwaters in oblique seas *Journal of Ocean Engineering and Technology* Vol. 15, No 2, pp. 22-33.
- Kee, S.T., Kim, J.K. and Han, J.O. (2001). "Interaction of triple porous-membranes with oblique seas", *International journal of ocean engineering and technology*, Vol. 4, No. 2, pp. 6-13.
- Kim, M.H. & Kee, S.T. (1996) "Flexible membrane wave barrier. Part 1. Analytic and numerical solutions" *ASCE J. of Waterway, Port, Coastal & Ocean Engineering*, Vol.122, No.1, 46-53.
- Thompson, G.O., Sollitt, C.K., McDougal, W.G. & Bender W.R. (1992) "Flexible membrane wave barrier" *ASCE Conf. Ocean V*, College Station, 129-148.
- Wang, K.H. & Ren, X. (1993), "Water waves on a flexible and porous breakwater" *Journal of Engineering Mechanics*, Vol.119, 1025-1048.

2001년 6월 19일 원고 접수  
2001년 7월 20일 최종 수정본 채택